Earth, Planets and Space

FRONTIER LETTER

Open Access

Forecasting the fate of vertically propagating dikes from geodetic data

Yosuke Aoki[1*]

Abstract

Magmas, especially mafic ones, usually intrude into the upper crust as dikes. The intruded dike is often arrested before reaching the surface to make an eruption. Many geophysical observations, including geodetic measurements, have documented dike intrusions and arrests. Also, many theoretical considerations and analog experiments explored the mechanics of dike propagation and arrest. However, insights gained from theoretical considerations, analog experiments, and geophysical observations have yet to be well reconciled. This study attempts to reconcile geodetic measurements with insights gained from theoretical considerations and analog experiments to investigate how to forecast whether an intruded dike results in an eruption or not. This study considers four causes of dike arrests: (1) solidification of the intruded magma, (2) insufficient volume of dike intrusion, (3) negative buoyancy acting on the intruded magma, and (4) stress perturbation near the dike tip by a large earthquake. Then, this study investigates the cause of dike arrests associated with the 1997 and 1998 seismic swarm off the Izu Peninsula, Japan, and the 2015 failed eruption of Sakurajima volcano, Japan, as an example. This study suggests that the dike intrusions associated with the 1997 and 1998 seismic swarm off the Izu Peninsula are caused by insufficient volume of the dike, the loss of buoyancy, or both. The failed eruption of the 2015 Sakurajima eruption is most likely by insufficient volume. To investigate the contribution of geodetic data in understanding the cause of dike arrests, it is essential to consider the characteristics of geodetic data. They are: (1) geodetic data constrain the intruded volume and the location relatively well, (2) geodetic data cannot constrain the geometry of the intruded dike very well, (3) an assumption of the host rock as homogeneous halfspace underestimates the volume of the intruded dike and estimates the depth of the dike shallower than the true value. These limitations indicate that we cannot fully understand the cause of dike arrests solely from geodetic data. Independent information gained from, for example, the location of dike-induced earthquakes, seismic structures, or density structure from gravity anomalies or muon radiography helps better understand the cause of dike arrests.

Keywords Dike propagation, Failed eruption, Buoyancy, Geodetic measurements

*Correspondence:
Yosuke Aoki
yaoki@eri.u-tokyo.ac.jp
Full list of author information is available at the end of the article

Graphical Abstract

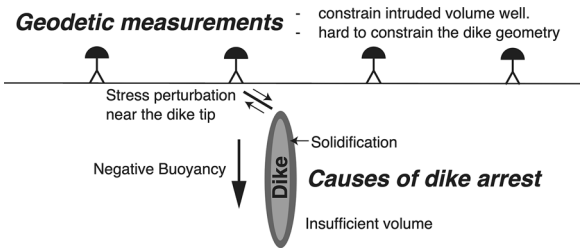

Introduction

In the upper crust of the Earth, magma often propagates as thin sheets. They are called dikes or sills when they propagate vertically or horizontally, respectively. Theoretically, dike or sill propagation is favored over propagation as diapir when the viscosity contrast between the magma and host-rock satisfy (Rubin 1993)

$$\left(\frac{\Delta p}{\mu}\right) > \left(\frac{\eta_m}{\eta_r}\right)^{1/3} \tag{1}$$

where η_m, η_r Δp, and μ represent magma viscosity, host-rock viscosity, magma overpressure, and host-rock rigidity, respectively. Because the left-hand side of eq. (1) is on the order of 10^{-4}, the viscosity contrast between magma and host rock needs to be 10^{-12} or smaller. Because the host-rock viscosity is usually 10^{18} Pa s or larger, basalt and andesite with low to intermediate viscosity, $\eta_m \leq 10^6$ Pa s propagate as dike or sill.

Dike propagation in active volcanoes has been ubiquitously observed. Recent examples include the 2021 Fagradalsjall, Iceland (Sigmundsson et al. 2022), 2021 Nyiragongo, Democratic Republic of the Congo (Smittarello et al. 2022), and 2018 Kīlauea, Hawai'i (e.g., Neal et al. 2019), eruptions. A dike propagation does not always result in an eruption but is often arrested before reaching the surface. For example, a dike intrusion in Sakurajima volcano, Japan, in 2015 generated significant deformation but did not result in an eruption (Hotta et al. 2016; Morishita et al. 2016). In fact, many intruded dikes are arrested, contributing to a volcano's growth. Therefore, it is essential to understand what controls the fate of an intruded dike not only for hazard assessment but also from a scientific viewpoint.

Despite its importance, an intruded dike's fate is not well forecasted. The main reason is that insights gained from theoretical, experimental, and observational studies are not reconciled well. The dynamics of dike propagation have been investigated for decades from theoretical and experimental aspects (e.g., Rubin 1995; Rivalta et al. 2015, for reviews) and geodetic and seismological observations (e.g., Aoki et al. 1999; Sigmundsson et al. 2022; Smittarello et al. 2022). However, no studies have considered how the monitoring data contributes to forecasting whether an intruded dike reaches the surface. This study investigates the cause of previous dike arrests from observational, theoretical, and experimental aspects, taking the 1997 and 1998 dike intrusions off the Izu Peninsula, Japan, and the 2015 failed eruption of Sakurajima Volcano, Japan, as an example of failed eruptions. Because both examples are related to subduction volcanism and under slightly extensional stress regimes, adding examples in different stress regimes, such as a more extensional regime like Iceland or the East African rift, would be a good idea. However, a more rigorous investigation with more examples is left for future study.

Theoretical consideration of dike arrest

Theoretical and experimental studies have shown that an arrest of an intruded dike is induced by (1) solidification of magma by cooling, (2) insufficient amount of intrusion, (3) negative buoyancy acting on magma, and (4) stress perturbation near the dike tip by an earthquake (e.g., Rubin 1995; Taisne et al. 2011; Rivalta et al. 2015; Maccaferri et al. 2016; Pansino et al. 2019). This section investigates each of them and assesses the causes of failed eruptions.

Solidification of magma

Magma intruded to shallow depths solidifies by being cooled by the host rock of a lower temperature. Whether magma is solidified by cooling is controlled by a nondimensional parameter Φ, or the inverse of the Fourier number, F_o, as

$$\Phi = \frac{1}{F_o} = \frac{Q\delta^2}{\alpha V} = \frac{\delta^2}{\alpha t} \tag{2}$$

where Q, V, δ, and α represent magma's flux, volume, thickness, and thermal diffusivity, respectively. Therefore,

$t = V/Q$ denotes the time of intrusion. Pansino et al. (2019) demonstrated by analog experiments that an intruded dike is arrested by solidification when $\Phi < 0.1$.

Figure 1 depicts the time for an intruded dike to freeze as a function of the dike thickness or $\Phi = 0.1$ in eq. (2). The figure shows that a dike with a thickness of 0.3, 1, and 3 m and a standard value of thermal diffusivity $\alpha = 10^{-6}\,\mathrm{m}^2/s$ (Vosteen and Schellschmidt 2003) freezes in $\sim 10^6$, 10^7, and 10^8 s, or ~ 10, 100, and 1000 days, respectively.

Insufficient amount of intrusion

The maximum length to which an intruded dike can extend, $L_{\max}$, is governed by considering the force balance between the elasticity and buoyancy as (e.g., Taisne et al. 2011)

$$\frac{\mu}{1-\nu}\frac{\delta}{L_{\max}} \sim \Delta\rho g L_{\max} \tag{3}$$

where μ, ν, $\Delta\rho$, and g represent rigidity, Poisson's ratio, the density difference between the magma and host rock, and the gravity constant, respectively. Equation (3) is rewritten as

$$L_{\max} \sim \left(\frac{\mu}{1-\nu}\frac{\beta V}{\Delta\rho g}\right)^{1/4} \tag{4}$$

where β denotes the ratio of the length L and width W of the dike (Fig. 2) as $\beta = L/W$. β is usually not far from 1. This study employs the opposite convention for the length and width of the dike compared to those used in the seismic and geodetic literature (e.g., Okada 1985; Aki and Richards 2002). For the intruded magma to make the surface or cause an eruption, $L_{\max}$ needs to be greater than the depth of the magma reservoir from which the dike initiates. In other words, V in eq. (4) denotes the minimum volume to cause an eruption, given the depth of the magma reservoir.

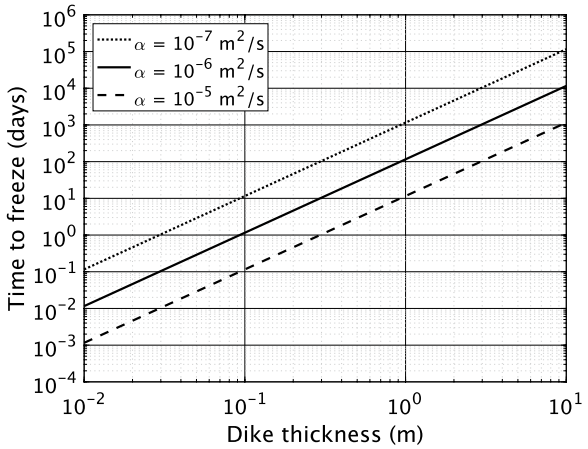

Fig. 1 The time for an intruded dike to freeze as a function of dike thickness with different thermal diffusivities

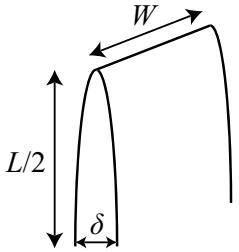

Fig. 2 Definition of length and width of an intruded dike. L, W, and δ represent the length of the dike in the vertical direction, that of the along-strike directions, and the width of the dike, respectively. The definition of L and W is the opposite of that commonly employed in seismological and geodetic communities

Figure 3 depicts the maximum length of a dike, $L_{\max}$, as a function of the intruded volume and density differences between the magma and host rock, given the aspect ratio of the dike as $\beta = 1$, the rock rigidity as $\mu = 10$ GPa, and Poisson's ratio as $\nu = 0.25$. While $L_{\max}$ is proportional to $V^{1/4}$ and $\Delta\rho^{-1/4}$, as eq. (4) indicates, it is mainly controlled by the intruded volume, V because the intruded volume V can vary by orders, while the density difference $\Delta\rho$ varies only by factors. In addition, while the aspect ratio of the intruded dike, α, can vary by factors, it does not affect $L_{\max}$ much because $L_{\max}$ is only proportional to $\beta^{1/4}$, as eq. (4) shows.

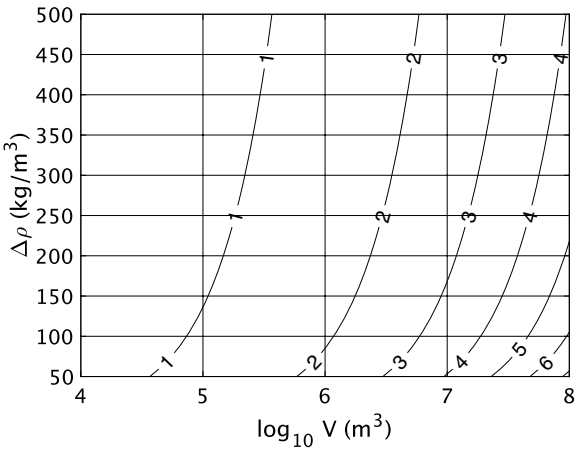

Fig. 3 The maximum dike length (in km), given the intruded magma volume, the density difference between the magma and host rock as a driver of positive buoyancy, aspect ratio $\alpha = 1.0$, rock rigidity $\mu = 10$ GPa, and Poisson's ratio $\nu = 0.25$. As eq. (4) indicates, the maximum dike length is proportional to $\alpha^{1/4}$. Therefore, a change of α by a factor of 2, for example, changes the maximum dike length as a factor of $2^{1/4} - 1.19$

Negative buoyancy

As has been discussed, the main driver of the vertical propagation of a dike is buoyancy. However, the intruded magma may lose buoyancy at some point because the density of the host rock decreases with decreasing depth.

Magma can propagate beyond the neutral buoyancy to some extent. Then, how long can a dike propagate beyond the neutral buoyancy? When the density of the host rock decreases monotonically with decreasing depth, the dike experiences the largest overpressure at a depth of neutral buoyancy because the dike at a depth of neutral buoyancy experiences the pressure by negative buoyancy from the dike above it. If we assume that the density difference between the host rock and magma is uniform as $\Delta\rho_+$ above the neutral buoyancy and the height of the dike above the neutral buoyancy is L_p, the overpressure at the neutral buoyancy is $g\Delta\rho_+ L_p$ (Taisne et al. 2011, Fig. 3), where g represents the gravity constant. This needs to be the tensile strength of rock ΔP_c as

$$\Delta P_c \leq g\Delta\rho_+ L_p. \tag{5}$$

A sill formation results when the overpressure by negative buoyancy exceeds a tensile strength at the level of neutral buoyancy (Fig. 3b). Equation (5) readily gives

$$L_p \leq \frac{\Delta P_c}{g\Delta\rho_+}. \tag{6}$$

L_p needs to be less than the depth of neutral buoyancy for an intruded dike to be arrested.

Figure 4 denotes L_p as a function of $\Delta\rho_+$ and ΔP_c. L_p is sensitive to both $\Delta\rho_+$ and ΔP_c, ranging between less than 1 km and ~10 km with given reasonable values of $\Delta\rho_+ = 100$–300 kg/m^3 and $\Delta P_c = 1$–10 MPa (e.g., Heap et al. 2021).

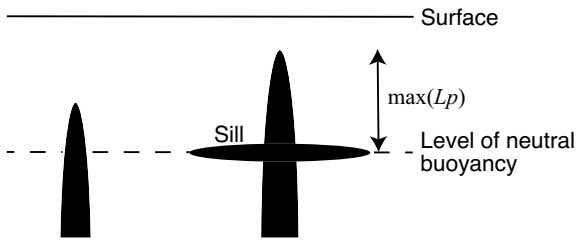

Fig. 4 Schematics of the dike propagation beyond the neutral buoyancy. (left) No sill formation because the magma overpressure is below the tensile strength of the host rock. (right) Sill formation because the magma overpressure reaches the tensile strength of the host rock. The sill is formed at the level of neutral buoyancy because the overpressure is maximum there. max(L_p) denotes the maximum length the intruded dike can reach beyond the level of neutral buoyancy

External forcing

Stress concentration at the dike tip, as well as positive buoyancy acting on the magma, is an important driving force for a propagating dike. A dike propagates when the stress intensity factor K

$$K = \sqrt{\frac{2\mu E}{1-\nu}} \tag{7}$$

reaches the critical value K_c, where E represents the fracture energy at the dike tip with a dimension of J.

Since stress perturbation by the dike intrusion is concentrated around the dike tip, dike-induced earthquakes are concentrated around the dike tip (e.g., Rubin and Gillard 1998). A dike-induced earthquake further perturbs the stress field, especially if it is large. If the dike-induced earthquake gives extensional stress perturbation at the dike tip, the fracture energy E increases; therefore, the stress intensity factor K increases, driving the dike to propagate further. On the other hand, if the dike-induced earthquake gives compressional stress perturbation, the fracture energy and stress intensity factor at the dike tip decrease. Therefore, this perturbation can make the stress intensity factor below the critical value, inhibiting further dike growth.

A typical example of a dike arrest by a large earthquake is the 2000 dike propagation of Miyakejima Volcano, Japan, although it is a horizontal dike propagation. Geodetic data indicates that the magma supply continues for about two months (e.g., Yamaoka et al. 2005; Murase et al. 2006; Akiyama et al. 2022), while earthquake locations suggest that the dike propagated only during the first week of the activity, followed by a thickening of a dike without propagation (e.g., Toda et al. 2002). Maccaferri et al. (2016) suggested with numerical simulations that stress changes near the dike tip by a M=6.5 earthquake inhibited further dike propagation. Vertical dike propagation can also be arrested by stress perturbations by a dike-induced earthquake.

Observation of dike arrests

A failed eruption by dike arrest is ubiquitous in active volcanoes (e.g., Moran et al. 2011). However, not many failed eruptions are well recorded by geophysical instruments. Here, three failed eruptions are taken as an example: the 1997 and 1998 seismic swarm off the Izu Peninsula, Japan, and the 2015 failed eruption of Sakurajima volcano, Japan. This section investigates what arrested the propagating dike during unrest.

The 1997 and 1998 seismic swarms off the Izu Peninsula

The eastern offshore of the Izu Peninsula, Japan, experienced seismic swarms in the 1980 s and 1990 s. Although the origin of the seismic swarms was not understood for a

while, a submarine eruption in 1989 confirmed that they were the volcanic origin. Okada and Yamamoto (1991) showed that the seismic swarm and associated ground deformation are mainly caused by dike intrusion. All the seismic swarms off the Izu Peninsula, except for the 1989 event, did not result in an eruption. Among them, the 1997 and 1998 seismic swarms are the most investigated because they are relatively large and have rich geodetic and seismic datasets.

The 1997 seismic swarm off the Izu Peninsula lasted for about 15 days. The associated seismicity concentrates between 3 and 10 km below sea level with gradual shallowing over time. Geodetic data allows us to image the propagating dike sub-vertically from ~7 to ~ 3 km during the seismic swarm. The total volume of intruded magma is approximately 1×10^7 m^3 (Aoki et al. 1999; Cervelli et al. 2001).

The 1998 seismic swarm off the Izu Peninsula has been investigated in more detail thanks to the enhanced seismic network. The seismic swarm continued for about a month, longer than the 1997 one. Hayashi and Morita (2003) relocated earthquakes associated with the seismic swarm to demonstrate that earthquakes are concentrated along the edge of a slightly inclined elliptical plane extending between ~4 and ~8 km below sea level. The observed earthquake distribution indicates that the earthquakes are generated by stress concentration near the tip of the dike with a dimension of ~4 km in the vertical and ~2 km in the horizontal direction. This observation is consistent with the theoretical consideration of dike-induced earthquakes by Rubin and Gillard (1998). Hayashi and Morita (2003) also delineated a linear seismicity between ~6 and ~8 km below sea level. This observation implies that the magma responsible for the seismic swarm came from depth. Morita et al. (2006) modeled the ground deformation associated with the seismic swarm by assuming that propagation of an elliptical dike outlined by hypocenters of the seismic swarm is mainly responsible for the observed ground deformation. They estimated the total intruded volume as approximately 3×10^7 m^3.

The 2015 failed eruption of Sakurajima Volcano

The 2015 failed eruption of Sakurajima Volcano is so far one of the best recorded failed eruptions with geophysical instruments, mainly with seismometers, tiltmeters, strainmeters, Global Navigation Satellite System (GNSS), and Synthetic Aperture Radar (SAR). Tilt and strain records indicate that the dike intrusion lasted for 1–2 days, but more than 90 % of the total volume intruded during the first 12 h and 60–70 % during the first 3 h (Hotta et al. 2016).

Volcano-tectonic earthquakes accompanied the dike intrusion. Precise relocation by Koike and Nakamichi (2021) shows that the seismicity continued for about 16 h. Seismicity is not as temporally concentrated within the first hours as deformation; 25–30 % of the total number of earthquakes occurred during the first 3 h. Approximately 40–50 % of total seismic energy, ~6.5×10^9 J or equivalent to $M_w \sim 3.1$, was released during the first 3 h. The volcano-tectonic earthquakes are vertically elongated with clusters at 0.2–1 km and 1.5 to −3.5 km below sea level. Geodetic data indicates that the shallower cluster emerged almost simultaneously with the onset of the dike intrusion. The deeper cluster started to emerge approximately 3 h after the onset of the dike intrusion (Koike and Nakamichi 2021). This seismic observation indicates that the intruded magma reached a depth of as shallow as 0.2 km below sea level.

This dike intrusion has been monitored by ~10 tiltmeters, 2 strainmeters, and ~20 GNSS antennas (Hotta et al. 2016). A tiltmeter and strainmeter detected a tilt change of more than 50 μrad and a strain change of more than 10 microstrains, respectively. GNSS measurements detected up to ~60 mm of horizontal displacements due to the intrusion. SAR images are taken from four different look angles to measure deformation. Morishita et al. (2016) detected more than 100 mm of horizontal displacements, more than 100 mm of uplift, and ~40 mm of subsidence at the volcano.

Hotta et al. (2016) modeled the observation by tiltmeters, strainmeters, and GNSS antennas as an intrusion of a southeast-dipping dike at 1.0 to −1.5 km below sea level, with an estimated volume of ~2.7×10^6m^3. Similarly, Morishita et al. (2016) modeled the InSAR measurements as an intrusion of a southeast-dipping dike at 0.4 to −1.2 km below sea level, with an estimated volume of the intruded dike is ~1.7×10^6m^3. At its maximum, the estimated volume flux was more than 100 m^3/s. Although both models fit well with the observation, they are inconsistent with seismicity. While both models favor a southeast-dipping dike, earthquakes do not have a dipping trend but align vertically. Also, the modeled dikes, ranging between 0.4 and 1.5 km below sea level (Hotta et al. 2016; Morishita et al. 2016), are shallower than earthquakes, ranging between 0.2 and 3.5 km below sea level (Koike and Nakamichi 2021). This discrepancy might be due to the ignorance of topography and heterogeneous, at least layered, crustal structure.

In addition, the dike geometry modeled from geodetic data gives the magma overpressure higher than the tensile strength. The magma overpressure Δp is given by $\Delta p \sim \mu\delta(L/W)^{1/2}$ where μ, δ, L, and W represent rigidity, thickness, length, and width of the dike, respectively (see "List of Symbols" in the revised manuscript).

Substituting $\mu = 10$ GPa and taking $\delta = 2$ m, $L = 2.3$ km, and $W = 0.6$ km from Hotta et al. (2016), the overpressure is given as $\Delta p \sim 20$ MPa, higher than the tensile rock strength of 1–10 MPa (Heap et al. 2021). Although this assessment is rough, itn suggests that the dike should be larger than Hotta et al. (2016)'s estimation. As the width is better constrained than the length, the dike should be longer than wider.

Observational constraints on the cause of dike arrests

What insights can geodetic and seismic observations give us into the mechanics of dike arrests? This section discusses the cause of the dike arrests by taking the seismic swarms off the Izu Peninsula in 1997 and 1998 and the 2015 failed eruption of Sakurajima as an example. The previous section outlines their observations. This section examines whether the dike arrest is caused by the solidification of magma, insufficient volume of the intruded dike, or negative buoyancy acting on the intruded magma.

The 1997 and 1998 seismic swarms off the Izu Peninsula

The discussion starts with whether the intruded dike is halted by solidification. Geodetic data indicates that the dike thickness is between 0.3–3 m (Aoki et al. 1999; Cervelli et al. 2001; Morita et al. 2006). While geodetic data can relatively constrain the intruded volume, constraining the geometry of the intruded body is more challenging. Therefore, the dike thickness is not very well constrained solely from geodetic data. Nonetheless, the dike thickness may be closer to 3 m, assuming the associated seismicity outlines the dike geometry (Hayashi and Morita 2003; Morita et al. 2006).

Then how much time does an intruded dike of a thickness of 3 m take to freeze? Substituting the dike thickness $\delta = 3$ m, time $t = 10$ days$= 8.64 \times 10^5$ s, and thermal diffusivity $\alpha = 10^{-6}$ m^2 (Vosteen and Schellschmidt 2003) into eq. (2) yields $\Phi \sim 120$. Since an intruded dike is solidified when $\Phi < 0.1$ (Pansino et al. 2019), solidification of the intruded dike may not have played a significant role. Equation (2) and Fig. 1 indicate that a dike of 3 m thick freezes in ~1000 days. As the intruded dike continued to thicken for 10–15 days, considering only the heat conduction as the driver of solidification is unjustified. Figure 1 and eq. (2) indicate that a dike of 0.3 m thick freezes in ~10 days. Therefore, the edge of the intruded dike, which is thinner than the center, may have been frozen during the intrusion. In that case, the frozen part prevents the still-molten part of the dike from propagating further.

Geodetic data can relatively constrain the intruded volume of the dike during the seismic swarms as $1–3 \times 10^7$ m^3 (Aoki et al. 1999; Morita et al. 2006). Substituting Poisson's ratio $\nu = 0.25$, rigidity $\mu = 10$ GPa, the density difference between the host rock and magma $\Delta\rho = 100$ kg/m^3, gravity acceleration $g = 9.8$ m/s^2, and the aspect ratio of the dike $\beta = 1$ into eq. (4) yields the maximum dike length $L_{\max}$ ~3.31 to −4.49 km, which is comparable with the dike length outlined by dike-induced earthquakes, while the dike length might be longer than the one outlined by the seismicity (Hayashi and Morita 2003). Therefore, insufficient volume should have played a role in arresting the intruded dike, but it is probably not the sole cause for the arrest. Morita et al. (2006) postulated that the dike intrusion started at a depth of ~10 km, leading to the dike length of ~6 km. However, we need to note that the bottom depth of the dike is usually hard to constrain; this case is no exception.

If the relocated dike-induced earthquakes outlining the intruded dike (Hayashi and Morita 2003) are assumed to be around the neutral buoyancy acting on the intruded magma, the excess length of the intruded dike beyond the neutral buoyancy, L_p [eq. (6)] is 1–3 km, which is reasonable by assuming plausible parameters (Fig. 5). However, we need to note that geodetic data cannot constrain L_p at all. Instead, the density of the host rock is, at least, required from other measurements such as seismic or gravity observations.

The 2015 failed eruption of Sakurajima volcano

As in the previous example, the discussion starts with whether the intruded dike is arrested by solidification. Geodetic data show that the thickness of the intruded dike is between 1 and 4 m (Hotta et al. 2016; Morishita et al. 2016). Earthquake relocation by Koike and Nakamichi (2021) suggests that the dike might be longer and

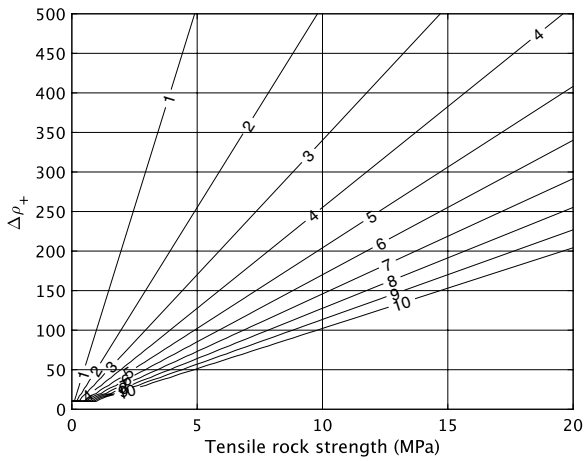

Fig. 5 The maximum dike length beyond the neutral buoyancy (in km) as a function of tensile rock strength and density differences between the intruded magma and the host rock, $\Delta\rho_+$

thinner than estimated by geodetic data. Reiterating the previous discussion, eq. (2) and Fig. 1 indicates that a dike of 3 m and 1 m thick freeze in ~1000 days and ~ 100 days with reasonable thermal diffusivity of $\alpha = 10^{-6}$ m^2. As the dike intrusion lasted for about 1/2 days in this case, the contribution of the solidification of magma should not have been dominant.

Hotta et al. (2016) and Morishita et al. (2016) indicate that the intruded volume during this failed eruption is between 1.7 and 2.7×10^6 m^3, about 1/10 of that by the seismic swarms off the Izu Peninsula that have been discussed in the previous section.

Substituting Poisson's ratio $\nu = 0.25$, rigidity $\mu = 10$ GPa, the density difference between the host rock and magma $\Delta\rho = 100$ kg/m^3, and gravity acceleration $g = 9.8$ m/s^2 into eq. (4) yields $L_{\max}$ as about 0.7 km. This value is smaller than the estimates by Hotta et al. (2016) and Morishita et al. (2016), which are between 1.5 and 4 km. A larger density contrast of $\Delta\rho = 500$ kg/m^3 gives $L_{\max} \sim 1.5$ km, marginally within the geodetic estimates. Therefore, insufficient volume may significantly contribute to this failed eruption but is not the sole contributor.

Assessing if this failed eruption was caused by the negative buoyancy acting on the intruded magma is challenging. Despite the precise relocation of earthquakes by Koike and Nakamichi (2021), it is challenging to constrain the height of the intruded dike beyond the negative buoyancy because earthquake locations do not show any particular features to indicate the level of neutral buoyancy.

An active seismic exploration indicates that the P-wave velocity beneath Sakurajima volcano is 2.3 to −2.8 km/s at 1 km below sea level or above (Miyamachi et al. 2013). An empirical relation between the P-wave velocity and density leads to the density of 2000–2100 kg/m^3 (Brocher 2005). Therefore, the density difference between the intruded magma and the host rock might be 400–500 kg/m^3 at most, leading to a short intrusion beyond the neutral buoyancy. While muon radiography derives high-resolution density structure beneath Sakurajima volcano at the shallowest depths (Oláh et al. 2018), it cannot derive density structure below sea level.

Discussion

The discussion in the previous sections shows that it is challenging to forecast whether a vertically propagating dike reaches the surface solely from geodetic data. This section discusses the requirement to better forecast the dike propagation.

As with other geophysical observations, ground deformation is measured at the surface or shallow subsurface, indicating that the observation is not sensitive to the detailed geometry of the intruded dike. Indeed, many studies indicated that while geodetic data constrain the volume of dike intrusion relatively well, the geometry of the intruded dike is not well constrained. In other words, there is a trade-off between the dike thickness, length, and width [see, for example, Fig. 8 of Hotta et al. (2016)]. Therefore, evaluating the contribution of magma solidification contains significant uncertainties since the dike thickness is a crucial parameter to evaluate it. If earthquake locations help constrain the geometry of the intruded dike, as with the case of the 1998 seismic swarm off the Izu Peninsula (Hayashi and Morita 2003), for example, the thickness of the dike is better constrained because the intruded volume is relatively well constrained from geodetic data and the dike geometry is constrained from seismicity. However, earthquake locations often do not play a perfect role in constraining the dike geometry.

Evaluating the role of negative buoyancy in arresting an intruded dike from geodetic data also contains significant uncertainties. Earthquake locations sometimes give some ideas about the propagating distance of the dike beyond the neutral buoyancy. For example, a ring-shaped seismicity associated with the 1998 seismic swarm off the Izu Peninsula (Hayashi and Morita 2003) implies that the dike propagated beyond the neutral buoyancy by the distance of the radius of the ring-shaped seismicity, approximately 4 km, or less. In many cases, however, earthquake locations do not help constrain the dike's length beyond the neutral buoyancy or the depth of neutral buoyancy because (1) earthquake locations are not always distributed to clearly outline the dike geometry and (2) earthquake locations do not provide any information about the density of the hot rock. Also, deformation data does not provide information about the density of the intruded dike or the host rock. Therefore, it does not contain any information about the density difference between the dike and the host rock, which is crucial to evaluate the distance by which the dike propagates beyond the neutral buoyancy [eq. (6)]. Constraining the host rock density requires gravity or seismic observations; the latter translates the seismic velocities to density through an empirical relation (Brocher 2005).

Given the intruded dike volume, which is well constrained from geodetic data, constraining the maximum possible dike length is relatively easy. Although there are uncertainties in the rock rigidity and the density difference between the dike and the host rock, the maximum length of the dike is proportional to these parameters only to the power of 1/4 (eq. (4)). As described earlier in this section, however, the length of the intruded dike is usually not well constrained solely from the geodetic data. Earthquake locations sometimes play a vital role in constraining the dike length, but not always.

Then, what improves the understanding of the mechanics of a dike propagation and better forecasts the fate of it? As discussed earlier, geodetic data well constrain the intrusion volume but do not constrain the geometry of the intrusion well because the measurements are made at or near the surface. It is, therefore, necessary to constrain the dike's geometry with other geophysical observations, such as earthquake locations, density distribution, or seismic velocities.

The argument so far is only concerned with the kinematics of dike propagation and is not concerned with its dynamics. To forecast the fate of an intruded dike or whether an intruded dike makes the surface cause an eruption, incorporating insights into the dynamics of dike propagation into observations is necessary. This approach was pioneered in the early 2010 s (e.g., Anderson and Segall 2011, 2013), but not many studies have taken this line of approach so far. Future methodological developments are desired to better understand and forecast an intruded dike's fate.

Conclusion

This study investigates how the fate of vertically intruded dike can be forecasted by combining insights gained from theoretical considerations, analog experiments, and geophysical observations. In particular, we explore the role played by geodetic data to understand the cause of dike arrest. We first identified three main causes of the dike arrest, which are (1) solidification of magma, (2) insufficient volume of dike intrusion, and (3) negative buoyancy acting on the intruded magma. We then took the 1997 and 1998 seismic swarm off the Izu Peninsula, Japan, and the 2015 failed eruption of Sakurajima volcano, Japan, as an example to understand the cause of the dike arrest. The dike intrusion associated with the 1997 and 1998 seismic swarm off the Izu Peninsula has likely been arrested by insufficient intrusion volume, negative buoyancy acting on the magma, or both. Similarly, the 2015 failed eruption of Sakurajima volcano has likely been caused by insufficient volume of magma or negative buoyancy acting on the magma. A caveat is that more than just geodetic data are required to understand the mechanics of dike propagation and unrest mainly because while geodetic data constrain the volume of the intruded magma well, the shape of the intruded dike is less well constrained. In other words, the thickness and length of the dike, which are essential parameters to assess the mechanics of dike propagation, are not well constrained because of trade-offs between each other. Therefore, independent information, including the location of dike-induced earthquakes to constrain the dike geometry and seismic and density structure to identify the depth of neutral buoyancy, is necessary to better address this problem.

Abbreviations

GNSS	Global Navigation Satellite System
SAR	Synthetic Aperture Radar
InSAR	Synthetic Aperture Radar Interferometry
E	Fracture energy at the dike tip (J)
F_o	Fourier number (No dimension)
g	Gravity acceleration (m /s^2)
K	Stress intensity factor (Pa m$^{1/2}$)
K_c	Critical stress intensity factor (Pa m$^{1/2}$)
$L_{\max}$	Maximum dike length (m)
L_p	Dike height above the neutral buoyancy (m)
Δp	Magma overpressure (Pa)
ΔP_c	Tensile strength of rock (Pa)
Q	Magma flux (m^3/s)
t	Time (s)
V	Magma volume (m^3)
W	Dike width (m)
β	Aspect ratio of the dike ($= L/W$) (No dimension)
δ	Dike thickness (m)
η_m	Magma viscosity (Pa s)
η_r	Host-rock viscocity (Pa s)
μ	Host-rock rigidity (Pa)
ν	Poisson's ratio (No dimension)
$\Delta\rho$	Density difference between the magma and host rock below the neutral buoyancy (kg /m^3)
$\Delta\rho_+$	Density difference between the magma and host rock above the neutral buoyancy (kg /m^3)
Φ	Inverse of the Fourier number $= (Q\delta^2)/(\alpha V) = \delta^2/(\alpha t)$ (No dimension)

Acknowledgements

I thank the previous and current Editor-in-Chief, Yasuo Ogawa and Takeshi Sagiya for an invitation to contribute to this journal. Comments by Editor Atsuko Namiki and two anonymous reviewers substantially improved the manuscript.

Author contributions

YA conceptualized the research and wrote the manuscript.

Data availability

No data is used in this study.

Declarations

Competing interests

The author declares no competing interests.

Author details

[1]Earthquake Research Institute, The University of Tokyo, Tokyo 113-0032, Japan.

Received: 30 October 2023 Accepted: 17 April 2024
Published online: 06 May 2024

References

Aki K, Richards PG (2002) Quantitative seismology. University Science Books, New York

Akiyama T, Kawabata H, Yoshioka S (2022) Spatiotemporal changes in fault displacements associated with seismovolcanic events in and around Miyakejima and Kozushima in 2000 inferred from GNSS data. Pure Appl Geophys 179:4245–4265. https://doi.org/10.1007/s00024-022-03084-y

Anderson K, Segall P (2011) Physics-based models of ground deformation and extrusion rate at effusively erupting volcanoes. J Geophys Res 116:B07204. https://doi.org/10.1029/2010JB007939

Anderson K, Segall P (2013) Bayesian inversion of data from effusive volcanic eruptions using physics-based models: application to Mount St. Helens 2004–2008. J Geophys Res 118:2017–2037. https://doi.org/10.1092/jgrb.50169
Aoki Y, Segall P, Kato T, Cervelli P, Shimada S (1999) Imaging magma transport during the 1997 seismic swarm off the Izu Peninsula, Japan. Science 286:927–930. https://doi.org/10.1126/science.286.5441.927
Brocher TM (2005) Empirical relations between elastic wavespeeds and density in the Earth's crust. Bull Seismol Soc Am 95:2081–2092. https://doi.org/10.1785/0120050077
Cervelli P, Murray MH, Segall P, Aoki Y, Kato T (2001) Estimating source parameters from deformation data, with an application to the March 1997 earthquake swarm off the Izu Peninsula, Japan. J Geophys Res 106:11217–11237. https://doi.org/10.1029/2000JB900399
Hayashi Y, Morita Y (2003) An image of a magma intrusion process inferred from precise hypocentral migrations of the earthquake swarm east of the Izu Peninsula. Geophys J Int 153:159–174. https://doi.org/10.1046/j.1365-246X.2003.01892.x
Heap MJ, Wadsworth FB, Heng Z, Xu T, Griffiths L, Valasco AA, Vairé E, Vistour M, Reuschlé T, Troll VR, Deegan FM, Tang C (2021) The tensile strength of volcanic rocks: experiments and models. J Volcanol Geotherm Res 418:107348. https://doi.org/10.1016/j.jvolgeores.2021.107348
Hotta K, Iguchi M, Tameguri T (2016) Rapid dike intrusion into Sakurajima volcano on August 15, 2015, as detected by multi-parameter ground deformation observations. Earth Planet Space 68:68. https://doi.org/10.1186/s40623-016-0450-0
Koike M, Nakamichi H (2021) Dike inflation process beneath Sakurajima volcano, Japan, during the earthquake Swarm of August 15, 2015. Front Earth Sci 8:600223. https://doi.org/10.3389/feart.2020.600223
Maccaferri F, Rivalta E, Passarelli L, Aoki Y (2016) On the mechanisms governing dike arrest: insight from the 2000 Miyakejima dike injection. Earth Planet Sci Lett 434:64–74. https://doi.org/10.1016/j.epsl.2015.11.024
Miyamachi H, Tomari C, Yakiwara H, Iguchi M, Tameguri T, Yamamoto K, Ohkura T, Ando T, Onishi K, Shimizu H, Yamashita Y, Nakamichi H, Yamawaki T, Oikawa J, Ueki S, Tsutsui T, Mori H, Nishida M, Hiramatsu H, Koeda T, Masuda Y, Katou K, Hatakeyama K, Kobayashi T (2013) Shallow velocity structure beneath the Aira caldera and Sakurajima Volcano as inferred from refraction analysis of the seismic experiment in 2008. Bull Volcanol Soc Jpn 58:227–237. https://doi.org/10.18940/kazan.58.1_227
Moran SC, Newhall C, Roman DC (2011) Failed magmatic eruptions: late-stage cessation of magma ascent. Bull Volcanol 73:115–122. https://doi.org/10.1007/s00445-010-0444-x
Morishita Y, Kobayashi T, Yarai H (2016) Three-dimensional deformation mapping of a dike intrusion event in Sakurajima in 2015 by exploiting the right-and left-looking ALOS-2 InSAR. Geophys Res Lett 43:4197–4204. https://doi.org/10.1002/2016GL068293
Morita Y, Nakao S, Hayashi Y (2006) A quantitative approach to the dike intrusion process inferred from a joint analysis of geodetic and seismological data for the 1998 earthquake swarm off the east coast of Izu Peninsula, central Japan. J Geophys Res 111:B06208. https://doi.org/10.1029/2005JB003860
Murase M, Irwan M, Kariya S et al (2006) Time dependent model of magma intrusion in and around Miyake and Kozu islands, central Japan in June-August 2000. J Volcanol Geotherm Res 150:213–231. https://doi.org/10.1016/j.jvolgeores.2005.02.005
Neal CA, Brantley SR, Antolik L et al (2019) The 2018 rift eruption and summit collapse of Kīlauea Volcano. Science 363:367–374. https://doi.org/10.1126/science.aav7046
Okada Y (1985) Surface deformation due to shear and tensile faults in a half-space. Bull Seismol Soc Am 75:1135–1154. https://doi.org/10.1785/BSSA0750041135
Okada Y, Yamamoto E (1991) Dyke intrusion model for the 1989 seismovolcanic activity off Ito, central Japan. J Geophys Res 96:10,361-10,376. https://doi.org/10.1029/91JB00427
Oláh L, Tanaka HKM, Ohminato T, Varga D (2018) High-definition and low-noise muography of the Sakurajima volcano with gaseous tracking detectors. Sci Rep 8:3207. https://doi.org/10.1038/s41598-018-21423-9
Pansino S, Emadzadeh A, Taisne B (2019) Dike channelization and solidification: Time scale controls on the geometry and placement of magma migration pathways. J Geophys Res Solid Earth 124:9580–9599. https://doi.org/10.1029/2019JB018191
Rivalta E, Taisne B, Bunger AP, Katz RF (2015) A review of mechanical models of dike propagation: schools of thought, results and future directions. Tectonophysics 638:1–42. https://doi.org/10.1016/j.tecto.2014.10.003
Rubin AM (1993) Dike vs diapirs in viscoelastic rock. Earth Planet Sci Lett 119:641–659. https://doi.org/10.1016/0012-821X(93)90069-L
Rubin AM (1995) Propagation of magma-filled cracks. Ann Rev Earth Planet Sci 23:287–336. https://doi.org/10.1146/annurev.ea.23.050195.001443
Rubin AM, Gillard D (1998) Dike-induced earthquakes: theoretical considerations. J Geophys Res 103:10,017-10,030. https://doi.org/10.1029/97JB03514
Sigmundsson F, Parks M, Hooper A et al (2022) Deformation and seismicity decline before the 2021 Fagradalsfjall eruption. Nature 609:523–528. https://doi.org/10.1038/s41586-022-05083-4
Smittarello D, Smets B, Barrière J et al (2022) Precursor-free eruption triggered by edifice rupture at Nyiragongo volcano. Nature 609:83–88. https://doi.org/10.1038/s41586-022-05047-8
Taisne B, Tait S, Jaupart C (2011) Conditions for the arrest of a vertical propagating dyke. Bull Volcanol 73:191–204. https://doi.org/10.1007/s00445-010-0440-1
Toda S, Stein RS, Sagiya T (2002) Evidence from the AD 2000 Izu islands earthquake swarm that stressing rate governs seismicity. Nature 419:58–61. https://doi.org/10.1038/nature00997
Vosteen HD, Schellschmidt R (2003) Influence of temperature on thermal conductivity, thermal capacity and thermal diffusivity for different types of rock. Phys Chem Earth 28:499–509. https://doi.org/10.1016/s1474-7065(03)00069-x
Yamaoka K, Kawamura M, Kimata F, Fujii N, Kudo T (2005) Dike intrusion associated with the 2000 eruption of Miyakejima Volcano, Japan. Bull Volcanol 67:231–242. https://doi.org/10.1007/s00445-004-0406-2

Publisher's Note